IEICE TRANS. COMMUN., VOL.E90–B, NO.1 JANUARY 2007

PAPER

Simulation and Design of a Very Small Magnetic Core Loop Antenna for an LF Receiver

Kazuaki ABE[†a)] ***and*** **Jun-ichi TAKADA**[††]**,** ***Members***

SUMMARY In this paper, we evaluated the characteristics of the magnetic core loop antenna that is used to receive long wave radio signals for time standards. To evaluate the receiving sensitivity of the antenna, we calculated the antenna factor of the magnetic core loop antenna by combining a magnetic field simulation and a circuit simulation. The simulation results are in good agreement with the results obtained from the experiments. We then investigated the optimization of the antenna shape, and showed the relation between the shape of the magnetic core and the receiving sensitivity.

key words: *magnetic core loop antenna, LF, time standard, antenna factor, magnetic field simulation*

1. Introduction

The radio controlled clock or watch, which receives standard radio waves, can always provide us with precise date and time. However, the radio controlled watch tends to have a larger size than the conventional one, because an antenna and a receiver are additionally needed within the watch. Thus we need to promote miniaturization of the antenna equipped in radio controlled watches for better design.

The standard radio wave which is operated at the low frequency (LF) region can reach 1000 km or more outdoor. But the electromagnetic field strength becomes weak in a reinforced concrete building, and therefore we need to improve the receiving sensitivity of the radio controlled watch.

There are two time standard radio stations in Japan, as shown in Table 1 [1]. The electric field strength is achieved larger than 50 dBμV/m in the whole territory of Japan, which means most of the radio controlled clocks and watches can theoretically receive the time signals. These stations broadcast digital time codes that contain the current minute, hour, date, year, and the day of the week at a rate of 1 bit per second.

Table 2 shows the carrier frequencies used by the time signal stations in other countries. Although each of the stations in the different countries provides a different code format of time standard, some models of radio controlled clocks and watches can be utilized in multiple countries, since the carrier frequencies and modulation schemes are similar among these countries.

Table 1 Characteristics of radio station JJY.

	Ohtakadoya-yama	Hagane-yama
Date service began	6/10/1999	10/1/2001
Location	Fukushima pref.	Saga pref.
Latitude,	37° 22' N,	33° 28' N,
Longitude	140° 51' E	130° 10' E
Altitude	790 m	900 m
Antenna type	Omni-directional	Omni-directional
Antenna height	250 m	200 m
Carrier power	50 kW	50 kW
Antenna efficiency	25% or more	45% or more
Carrier frequency	40 kHz	60 kHz
Frequency accuracy	$\pm 1 \times 10^{-12}$	$\pm 1 \times 10^{-12}$

Table 2 Radio time signal stations.

Country	Station Call Sign	Carrier Frequency
Japan	JJY	40 kHz, 60 kHz
United States	WWVB	60 kHz
United Kingdom	MSF	60 kHz
Germany	DCF77	77.5 kHz
China	BPC	68.5 kHz

The purpose of this study is to establish a simulation technique for evaluating and designing magnetic core loop antennas (MCLAs) in radio controlled watches. Conventionally the evaluation has been done by a trial production and an experiment. By using electromagnetic simulations, we can rapidly investigate the optimal design of MCLAs. MCLAs have been used for a long time. However, the number of literatures treating MCLAs is very limited. References [2] and [3] expressed the received voltage of a ferrite rod antenna by using the shape parameters. They present approximate equations from the equivalent circuits of the antennas. However, the literatures that investigate the techniques for miniaturization and performance simulation of such antennas are quite seldom especially for LF. Therefore, it is important to discuss about the simulation process of MCLAs.

This paper is organized as follows. Section 2 introduces the basic character of straight magnetic core loop antenna. In Sect. 3, the simulation model of an MCLA and the simulation technique are explained. In Sect. 4, the measurement method for receiving sensitivity of the MCLA is described. In Sect. 5, the results of electromagnetic simulation and measurement of the prototype MCLAs are shown. The optimum design of the MCLA for LF is also discussed. Finally, the conclusion is given in Sect. 6.

Manuscript received February 1, 2006.
Manuscript revised May 15, 2006.

[†]The author is with the Advanced Research Laboratory, Hamura R & D Center, CASIO Computer Co., Ltd., Hamura-shi, 205-8555 Japan.
[††]The author is with the Graduate School of Science and Technology, Tokyo Institute of Technology, Tokyo, 152-8550 Japan.
a) E-mail: abe@rd.casio.co.jp

DOI: 10.1093/ietcom/e90–b.1.122

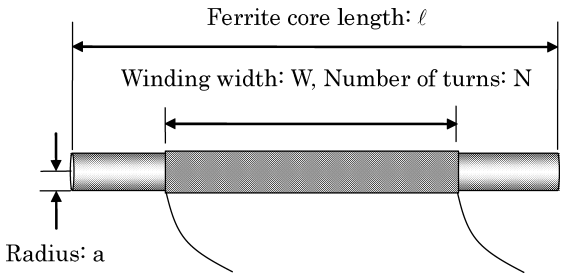

Fig. 1 Specification of the fabricated antennas.

2. MCLA

A solenoidal coil that is wound up to a magnetic core, shown in Fig. 1, is used for the antenna for LF time standard receiver. It is called an MCLA, or a bar antenna. If winding width of a coil is very long, the inductance of an MCLA is approximately written as follows assuming the uniform magnetic flux concentration in the core [4].

$$L = \mu \cdot \frac{\pi a^2 N^2}{W}, \tag{1}$$

where μ is the permeability of the magnetic core. But the calculation result of this equation is inaccurate in the case of small MCLAs, because the magnetic flux density in the core is not uniform due to the leakage near the ends of the coil. Furthermore, the shape of the magnetic core is not considered in Eq. (1). Thus even for calculating inductance of such a simple MCLA, an electromagnetic simulation is needed.

3. Simulation Model

The length of MCLAs used in the radio controlled watch is about 20 mm, even though the wavelength of receiving radio wave is several kilometers. For such electrically extremely small antennas, it is not appropriate to use an electromagnetic simulator used for the simulation of ordinary antennas. Instead, we considered such an MCLA as a magnetic field sensor and used a magnetic field simulator which is used for the electromechanical analysis. Such a simulator can handle the magnetic material and the eddy current in the LF region.

3.1 Inductance and Q-Factor

As a simulation tool for an MCLA, we used ANSOFT Maxwell 3D [5]. It is based on the finite element method (FEM), and generally used for magnetic field simulation in low frequency. At first, we input the shape of the MCLA into the simulator. The simulator can calculate the inductance of a single-turn coil. The inductance of an antenna is obtained by multiplying the simulation result by the squared number of turns of the coil.

It is important to evaluate the quality factor (Q-factor) of antennas, because the Q-factor has a close relation to the receiving sensitivity. However, the simulator could not simulate the Q-factor of the antenna directly. To evaluate the Q-factor, we derived an approximation formula from the equivalent circuit shown in Fig. 2. In the equivalent circuit on the left, R_w and R_m correspond to copper loss and core loss, respectively. The core loss includes hysteresis loss, eddy current loss, and residual loss. The copper loss is expressed as a series connection, while the core loss is expressed as a parallel connection. Actually an antenna coil has several picofarads of floating capacitance, but the Q-factor is not strongly affected by the floating capacitance in the low frequency region.

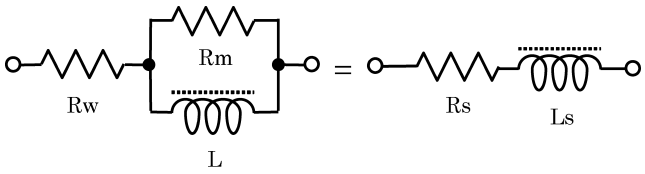

Fig. 2 The equivalent circuit of small MCLAs.

In the equivalent circuit on the right, the Q-factor is defined as

$$Q = \frac{\omega L_s}{R_s}. \tag{2}$$

From Eq. (2) the Q-factor of the equivalent circuit can be approximated as follows.

$$Q = \frac{1}{\dfrac{R_w}{\omega L} + \dfrac{\omega L}{R_m}\left(1 + \dfrac{R_w}{R_m}\right)} \cong \frac{1}{\dfrac{R_w}{\omega L} + \dfrac{\omega L}{R_m}}, \tag{3}$$

where $R_w \ll R_m$ is assumed. Although this assumption may not always be valid, it is adequate for the magnetic core that we evaluated in Sect. 5.2. In Eq. (3), the second term of the denominator is the loss factor of the magnetic core, $\tan\delta_m$. Since the core loss varies with the shape of the magnetic body, we approximately altered the equation using apparent permeability, μ_{app}, as follows.

$$Q = \frac{1}{\dfrac{R_w}{\omega L} + \tan\delta_m} \cong \frac{1}{\dfrac{R_w}{\omega L} + \left(\dfrac{\tan\delta}{\mu_i}\right) \cdot \mu_{app}}, \tag{4}$$

where $\tan\delta/\mu_i$ is the relative loss factor of the core material, which we can know from the data sheet of the magnetic core material. The initial permeability μ_i is the limiting value of permeability when the magnetic field strength is vanishingly small. In Eq. (4), we use apparent permeability not initial permeability, because the flux leakage cannot be ignored in an MCLA which is not a closed magnetic circuit. The apparent permeability is defined as the ratio between the inductance of the coil attached to the core (L) and that of the coil itself (L_0). That is,

$$\mu_{app} \equiv \frac{L}{L_0}. \tag{5}$$

The inductances L and L_0 are calculated by magnetic field

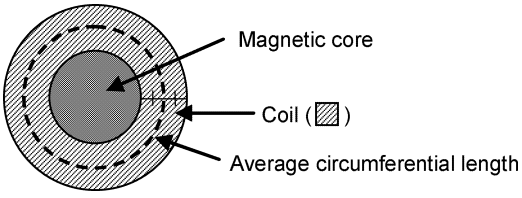

Fig. 3 Average circumferential length.

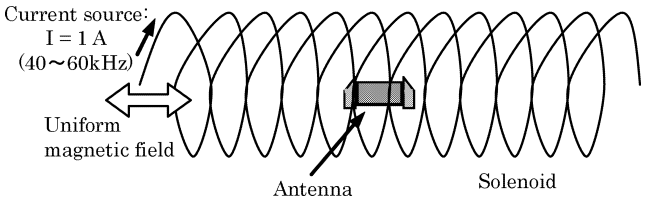

Fig. 4 Simulation model for antenna factor of the MCLA.

simulation, hence the apparent permeability can be obtained by Eq. (5).

In Eq. (4), the winding resistance R_w is expressed as

$$R_w = \rho \frac{\ell}{A}, \tag{6}$$

where ρ is the resistivity of copper, ℓ is the length of the coil, and A is the cross section of the coil. The length of the coil can be obtained by multiplying the average circumferential length to the winding number N. The average circumferential length is defined as shown in Fig. 3. Then we can obtain the Q-factor of the antenna by calculating Eq. (4).

3.2 Antenna Factor

Antenna factor is defined by the ratio of the electric field strength (E) to the received voltage (V_o) of the antenna as follows.

$$AF\,[\mathrm{dB/m}] = 20 \log \left[\frac{E}{V_o} \right]. \tag{7}$$

We evaluated the receiving sensitivity of an MCLA by the antenna factor. It is noted that an antenna factor is an easier and a more realistic parameter than the antenna gain for an MCLA, as the impedance is not usually matching between the receiver IC and the antenna in the low frequency system. To obtain the antenna factor, we have to generate a uniform magnetic field in a simulation model. Therefore we put the receiving antenna at the center of a solenoid, as shown in Fig. 4. An equivalent circuit of this simulation model is shown in Fig. 5. The left side section corresponds to the transmitting system, and the right side section corresponds to the receiving system. R_1, R_2, C_f, C_t and R_L correspond to the loss resistance of the transmit solenoid, the loss resistance of the receiving antenna, the floating capacitance of receiving antenna, the tuning capacitance and the input resistance of the receiver, respectively. The receiving sensitivity is related to a coupling constant (k), which is defined using the solenoid inductance (L_1), the receiving antenna (L_2), and the mutual inductance (M_{12}), as follows.

$$k \equiv \frac{M_{12}}{\sqrt{L_1 L_2}}. \tag{8}$$

It is possible to calculate the coupling constant using the electromagnetic simulator because the simulation model for antenna factor has two coils. But we cannot obtain the voltage at the resonance point directly because it includes a tuning capacitor.

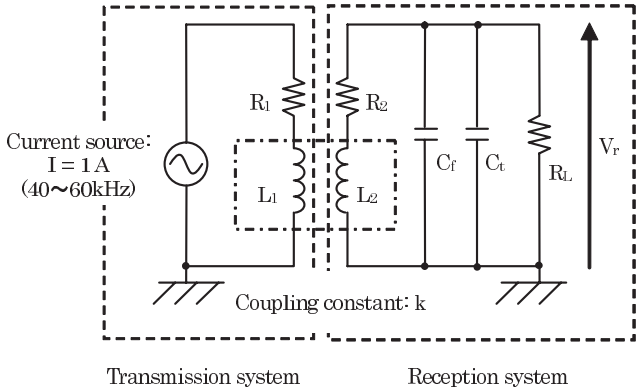

Fig. 5 Equivalent circuit of the simulation model for antenna factor of the MCLA.

Therefore, we took the following procedures to obtain the antenna factor. First we calculated the magnetic field strength and the coupling constant with the electromagnetic simulator. Equivalent TEM (plane wave) Electric field strength is obtained by multiplying wave impedance, 120π to the magnetic field strength. Then the received voltage at the resonance frequency was derived by a SPICE circuit simulator. Finally, we obtained the antenna factor of the receiving MCLA from Eq. (7).

4. Measurement Method for MCLAs

We measured the inductance and the Q-factor with the impedance analyzer (HP4194A). The magnetic characteristics of the core material varies with temperature, therefore, constant temperature room is necessary for the accurate measurement.

The MCLA is considered as an infinitesimally small magnetic dipole antenna. The antenna efficiency is very low, and it is not used as transmitting antenna. It is not possible to evaluate the antenna performance in the ordinary manner by using the standard dipole antenna in high frequency region, because the wavelength in LF region is reached at several kilometers. On the other hand, an antenna factor is generally used as the characteristic of antennas in EMC (Electro-Magnetic Compatibility). By using a standard antenna for the EMC measurement, the antenna factor of which is already known, we can evaluate the antenna factor of the MCLA.

We measured the antenna factor of the MCLA by using the substitution method to evaluate the receiving sensitivity. The measurement flow is as follows: 1) measure the electric

field strength (E) at the receiving position by using a standard loop antenna for EMC; 2) measure the received voltage (V_o) of MCLA at the same receiving positions where the standard loop antenna was located; 3) derive the antenna factor from Eq. (7).

When the receiving electric field strength was much less than 50 dBμV/m, the influence of noise from instruments and fluorescent lights became dominant. Therefore, we controlled the transmitting power to obtain the sufficient signal to noise ratio.

Figures 6 and 7 show the measurement systems of the antenna factor for the MCLAs. A continuous wave of 40 kHz or 60 kHz was used in the measurement from the signal generator. The low-frequency wave was transmitted by the loop antenna on the left, and received by the standard loop antenna on the right as shown in Fig. 6. As the antenna factor of the standard receiving antenna is already known, we can measure the equivalent received electric field strength by using a test receiver. Actually as a loop antenna detects a magnetic field, electric field strength is obtained by multiplying wave impedance and magnetic field strength.

After measuring the equivalent electric field strength, we replaced the receiving loop antenna with the MCLA at the same position as shown in Fig. 7. The axis of the ferrite core was placed normal to the plane of the transmitting loop antenna with the center of the ferrite core in the plane of the transmitting loop [6]. A buffer amplifier was used between the antenna and the instruments to avoid the influence of the cables. The receiving voltage was measured with a lock-in amplifier. A lock-in amplifier was used for very small signals with poor SNR. Its main function is to synchronize the input signal with the transmitted signal, and then filters the signal to a very narrow bandwidth. The received voltage of the MCLA is obtained by dividing the output voltage of the lock-in amplifier by the gain of the buffer amplifier.

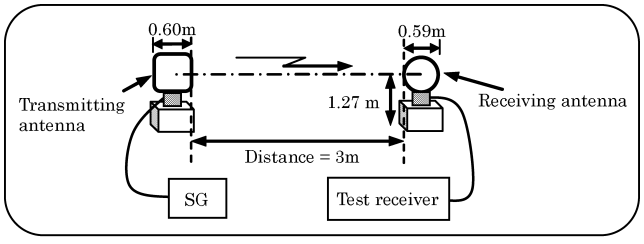

Fig. 6 Measurement of standard loop antenna.

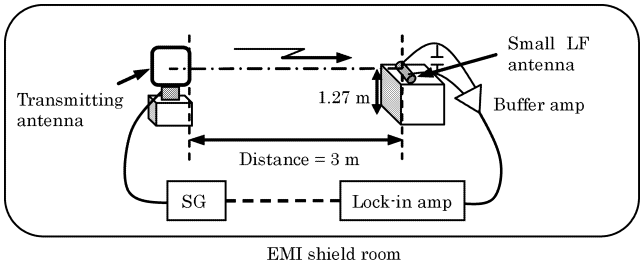

Fig. 7 Measurement of MCLA.

5. Simulation Results

5.1 Bar Shaped MCLA

The shape parameters of the prototype antennas are listed in Table 3. These parameters were chosen based on the MCLA used in radio controlled watches (antenna length = 16 mm, winding width = 11 mm) as described in Sect. 5.2. Figure 8 shows the prototype antennas. The magnetic core length is varied from 16 mm to 50 mm. The winding width is 11 mm or 5.5 mm, and the winding number of turns is 103 turns or 770 turns. These ranges of the parameters were chosen by considering the mechanical strength of the material and the winding coil thickness.

Characteristics of the core material used in Fig. 8, manganese zinc ferrite, are listed in Table 4. The initial permeability is 2400. We calculated the inductance of the bar shaped MCLA by magnetic field simulation.

Figures 9–11 illustrate the simulation results of the antenna inductance at 40 kHz. Each of the measurement points corresponds to the prototype number in Table 3. The inductance versus the core length is plotted in Fig. 9. When the ferrite core length is longer, the simulation error becomes larger, since the distribution of the magnetic flux in the air increases. However, this kind of error is not practically a problem, because our purpose is to design the small anten-

Table 3 Parameters of the prototype antennas.

Prototype No.	Core size: ϕ, ℓ	Winding parameters: diameter, W, N
1	1.1 mm, 16 mm	0.08 mm, 11 mm, 103 turns
2	1.1 mm, 16 mm	0.08 mm, 5.5 mm, 103 turns (double-layered)
3	1.1 mm, 16 mm	0.08 mm, 11 mm, 770 turns
4	1.1 mm, 24 mm	0.08 mm, 11 mm, 103 turns
5	1.1 mm, 36 mm	0.08 mm, 11 mm, 103 turns
6	1.1 mm, 50 mm	0.08 mm, 11 mm, 103 turns
7	1.1 mm, 50 mm	0.08 mm, 11 mm, 370 turns
8	1.1 mm, 50 mm	0.08 mm, 11 mm, 570 turns

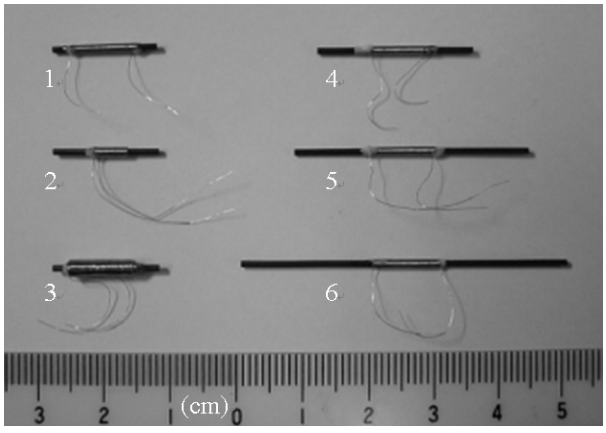

Fig. 8 Picture of the prototype antennas (Type A).

Table 4 Parameters of ferrite core for the prototypes.

Characteristics	Test condition	Value
Initial permeability: μ_i	23°C	2400
Saturation flux density: B_s	23°C	490 mT
Residual flux density: B_r	23°C	140 mT
Coercive force: H_c	23°C	12 A/m
Relative loss factor: $\tan\delta/\mu_i$	40 kHz	3.0×10^{-6}
Curie temperature: T_c	-	> 200°C
Electrical resistivity: ρ	-	5 Ωm

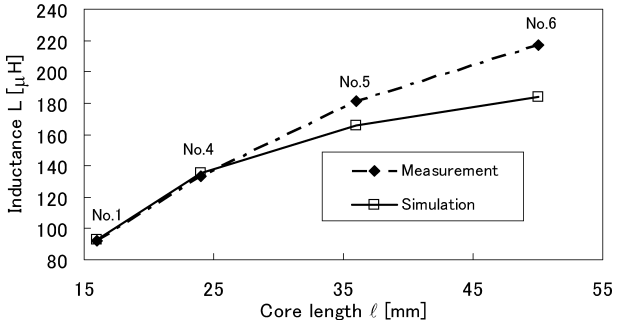

Fig. 9 Measurement and simulation results with respect to the relation between core length and inductance (Type A).

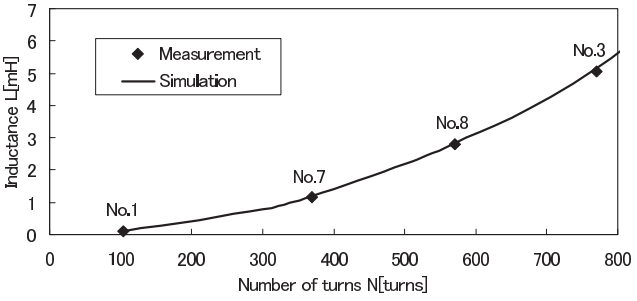

Fig. 10 Measurement and simulation results with respect to the relation between winding number of the coil and inductance (Type A).

nas for radio controlled watches. The inductance versus the winding number of the coil is plotted in Fig. 10. The solid line represents the product of the inductance of a single-turn coil by the squared number of turns of the coil. The figure reveals that the measured results are on the line of the simulation results. The inductance versus the winding width of the coil is plotted in Fig. 11. Only two points could be measured considering the uniformity of winding coil density. The simulation results are in good agreement with the measured values.

5.2 MCLA for Radio Controlled Watches

Figure 12 is a picture of an MCLA module used in the product radio controlled watches, while Fig. 13 shows simulation model of the MCLA used in the product (Type B).

The antenna length is 16 mm, and the winding number of turns is 1107. The copper wire with the diameter of 80 μm forms the coil. The magnetic body is covered with plastic for reinforcement. In the figure, a Flexible Printed

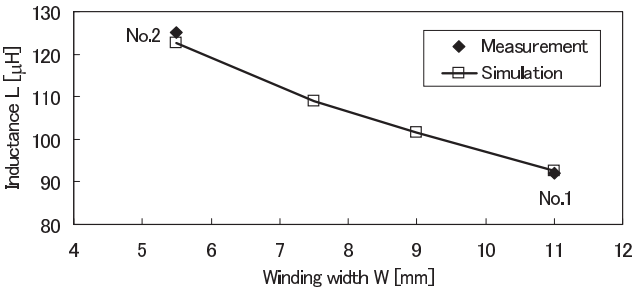

Fig. 11 Measurement and simulation results with respect to the relation between winding width of the coil and inductance (Type A).

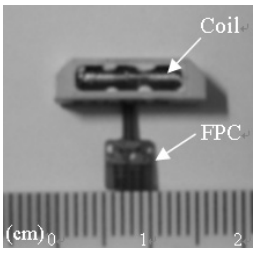

Fig. 12 The actual MCLA used in radio controlled watches.

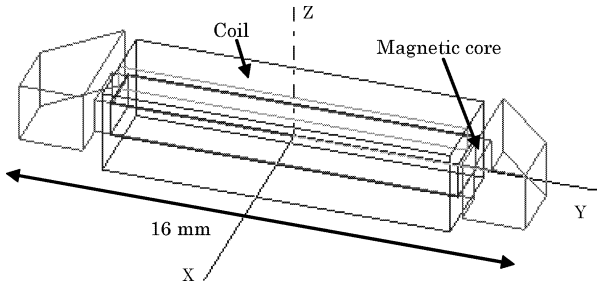

Fig. 13 Simulation model of the MCLA used in the product (Type B).

Table 5 Parameters of ferrite core (Mn-Zn ferrite).

Characteristics	Test condition	Value
Initial permeability: μ_i	23°C	8000
Saturation flux density: B_s	23°C	400 mT
Residual flux density: B_r	23°C	200 mT
Coercive force: H_c	23°C	5.6 A/m
Relative loss factor: $\tan\delta/\mu_i$	40 kHz	35×10^{-6}
Curie temperature: T_c	-	> 120°C
Electrical resistivity: ρ	-	0.05 Ωm

Circuit (FPC) to implement a tuning capacitor is connected to the antenna. Table 5 shows the characteristics of the core material. The permeability of the core is 8000.

We compared the simulation results with the measurements. Figures 14 and 15 show the inductance and Q-factor of the antenna at the frequencies of 40 kHz and 60 kHz respectively. The solid lines are the simulation results of the inductance and dashed lines are that of Q-factor. From these figures, we can see that the simulation results of inductance and Q-factor are in good agreement with the measurements.

Figure 16 shows the measurement values and the simulation results of the antenna factor within the frequency

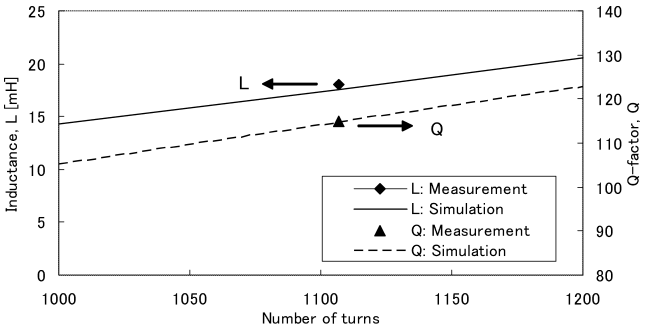

Fig. 14 Inductance and Q-factor of the MCLA, f = 40 kHz (Type B).

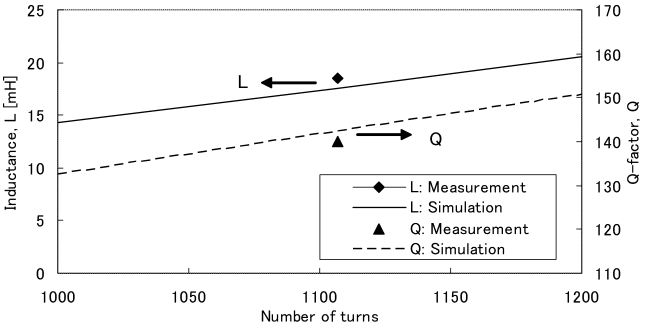

Fig. 15 Inductance and Q-factor of the MCLA, f = 60 kHz (Type B).

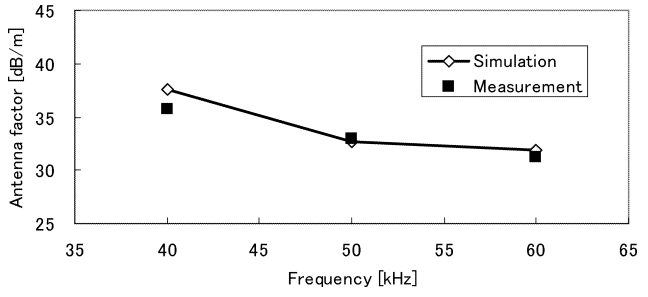

Fig. 16 Antenna factor of the MCLA (Type B).

range from 40 kHz to 60 kHz. The maximum difference between the simulation results and the measured values is 2 dB. Thus, it was confirmed that our procedure to derive the antenna factor is reasonably accurate. The antenna factor at 60 kHz is smaller than that at 40 kHz. This is because the Q-factor at 60 kHz takes larger values than that at 40 kHz.

5.3 Antenna Design for the Downsizing and the Receiving Sensitivity Improvement

A small antenna for radio controlled watch has the dumbbell shaped magnetic body, both ends of which concentrate magnetic flux into the coil. We call them lead parts. To confirm this concentration effect, we simulated the antenna factor with different shapes of lead parts. In Fig. 17, the cross sectional area of the lead parts is varied with the length parameter *D*.

Figure 18 shows the simulation results of the antenna

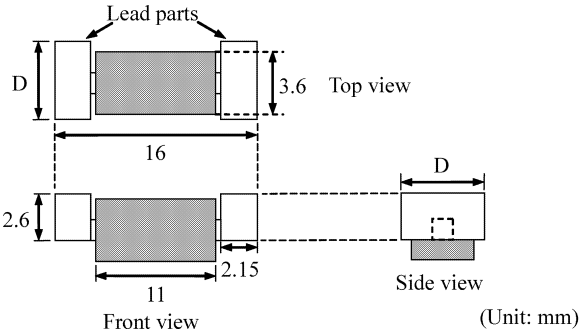

Fig. 17 Antenna model for the simulation (Type C).

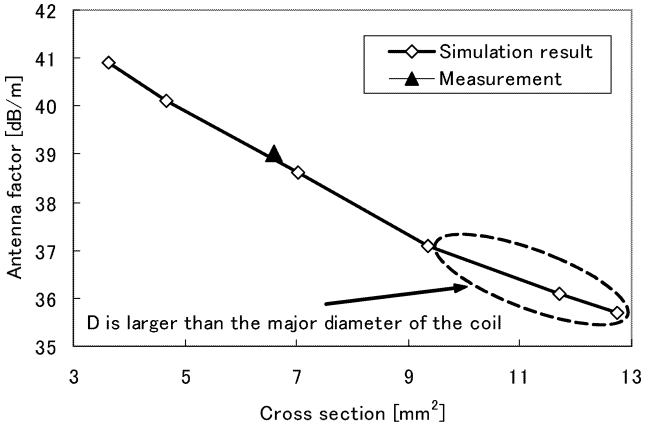

Fig. 18 Antenna factor vs. cross section (Type C).

factor versus the cross sectional area at a frequency of 40 kHz. The definition of the antenna factor implies that smaller antenna factor corresponds to higher receiving sensitivity. We see from Fig. 18 that the receiving sensitivity is improved as the size of the cross sectional area becomes larger. A triangular point corresponds to a measurement value of the product antenna for radio controlled watch. Though the shape of the antenna is different from simulation models, the measured antenna factor is on the straight line of the simulation results by applying the average cross sectional area.

The results reveal a discontinuity at the cross section of 9.4 mm^2. The discontinuity point occurs when the length D is equal to the major diameter of the coil. Figure 19 shows the simulation results of the magnetic field vector in this case. Figure 20 is the result in the case when the length D is larger than the major diameter of the coil. The external magnetic field comes from the positive y direction in both figures. In Fig. 20, we can see the antenna receives more magnetic flux than that in Fig. 19 because of a larger cross sectional area. However, the magnetic flux from the coil side, which is in opposite direction to the external magnetic flux, also increased in Fig. 20. The larger cross section than the major diameter of the coil means a loss for receiving sensitivity. Therefore, considering a small and efficient antenna, it was found that the size of lead part should be substantially the same as the major diameter of the coil [7].

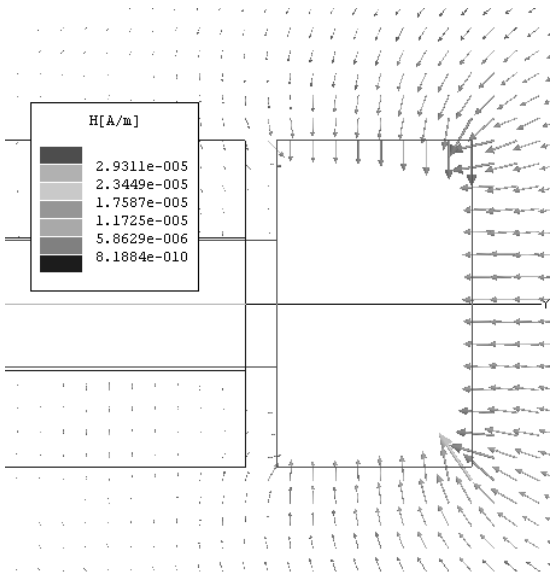

Fig. 19 Magnetic field vector when the length, D = 3.6 mm (Type C).

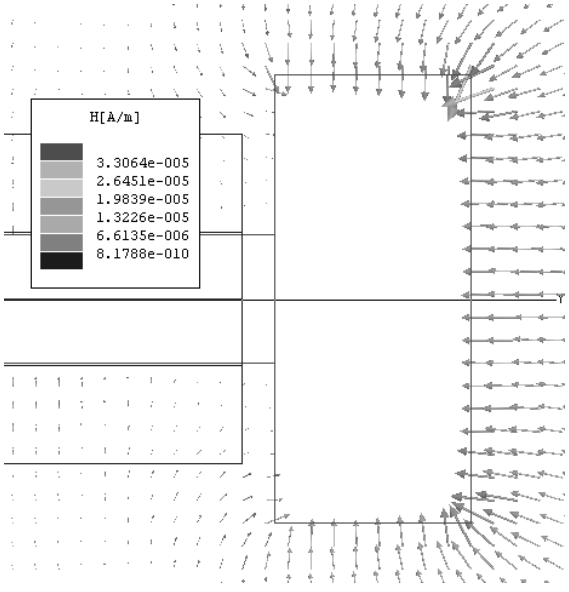

Fig. 20 Magnetic field vector when the length, D = 4.9 mm (Type C).

Table 6 Simulation parameters.

Frequency	40 kHz
Magnetic field strength	2.65 μA/m
Permeability of the magnetic core	8000
Conductance of the magnetic core	25 S/m
Volume of lead part (one part)	17.12 mm^3

As the next step, we analyzed the concentration of magnetic flux from the lead part of the magnetic body to find the optimum shape of antenna by simulation. Table 6 shows the simulation parameters that we investigated.

Figure 21 illustrates the simulation result of the magnetic flux density vector that flows from the lead part to inside the coil. We see from the figure that the magnetic flux

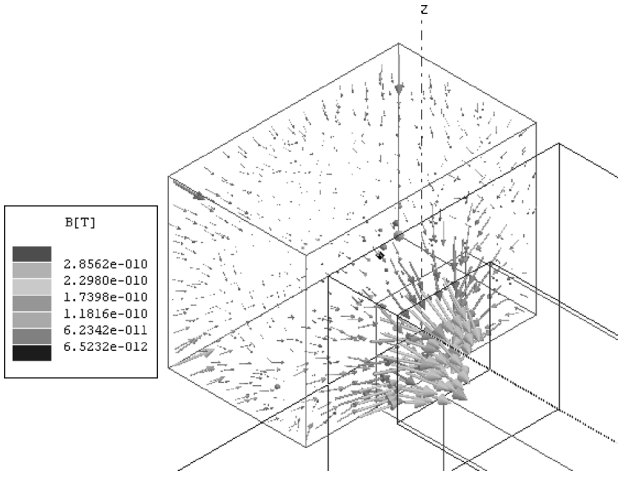

Fig. 21 Magnetic flux density gathering into the coil (Type C).

density is concentrated at the center of the magnetic core. The magnetic flux inside the coil (Φ) is obtained by integrating the normal component of the magnetic flux density (B_n) in the cross sectional area as Eq. (9),

$$\Phi = \int_{\mathrm{core}} B_\mathrm{n}\, dS. \tag{9}$$

Figure 22 shows the antenna models we evaluated. The cross sectional area and the length of the lead part are changed, while the volume of the lead part is constant. By this simulation we investigated the relationship between the shape of the magnetic body and the magnetic flux inside the coil.

Figure 23 shows the simulation results. (a)–(h) on the graph correspond to the shapes in Fig. 22. The MCLA simulation model of the "Products" referred in Fig. 23 is shown in Fig. 13. Larger magnetic flux corresponds to better receiving sensitivity, which can be deduced by Faraday's law of induction. These results revealed that magnetic flux is larger when the antenna length is longer, or the cross sectional area of lead parts is larger, as seen in models (h) and (a), respectively. The magnetic flux of a product antenna of a radio controlled watch shown as the triangular point, is approximately the same as model (e). The product antenna does not have long length or large cross sectional area, therefore the converged magnetic flux is not so large. On the other hand, a trapezoidal pillar shaped antenna achieves small size and higher dense magnetic flux showed as the square point. Figure 24 shows the magnetic flux density inside the trapezoidal shaped antenna. The magnetic flux is increased about 15% in comparison with model (e). One of the reasons for the improvement is that the shape of the magnetic body is along the route of the magnetic flux, which means reducing magnetic resistance. Another reason is that the cross sectional area of both ends is increased [8].

As another aspect of MCLAs, we focus on the magnetic flux distribution inside the antenna core. Figure 25 shows an example of the magnetic flux density inside the coil of the MCLA calculated using electromagnetic simula-

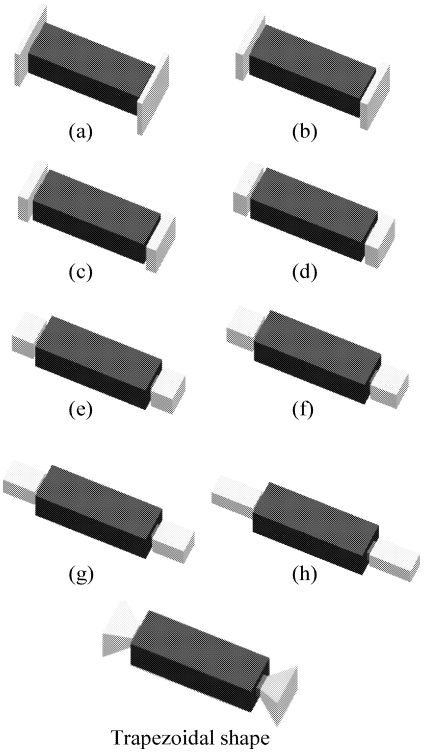

Fig. 22 Antenna models for the simulation.

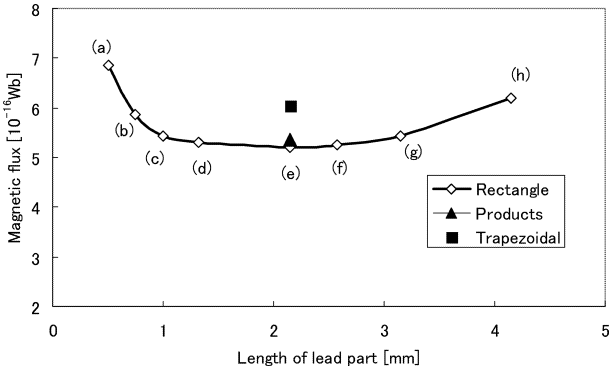

Fig. 23 Simulation results of magnetic flux.

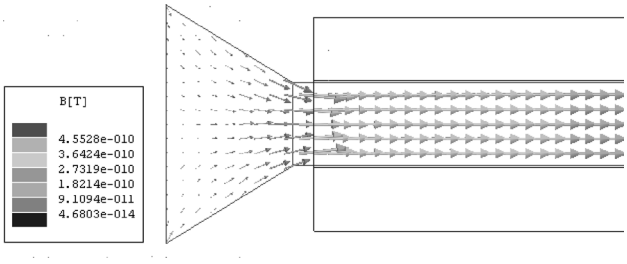

Fig. 24 Magnetic flux density of trapezoidal shaped antenna.

tion. The figure reveals how the magnetic flux density becomes higher as the observation point is closer to the center of the antenna core. The distribution of the magnetic flux inside the antenna core is obtained by integrating the mag-

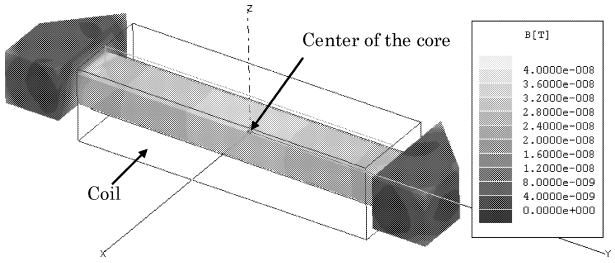

Fig. 25 Magnetic flux density inside the antenna coil (Type B).

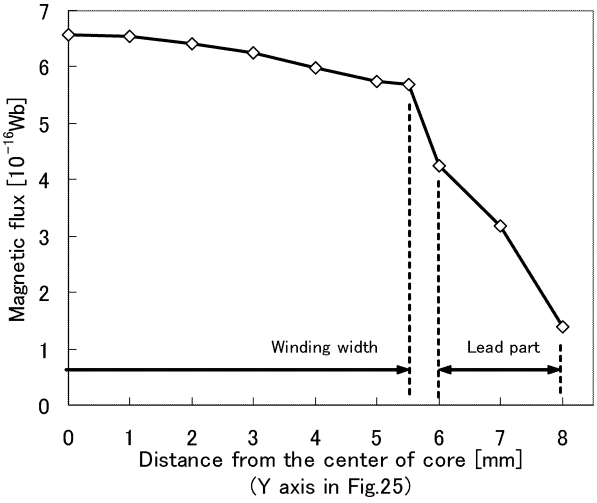

Fig. 26 Magnetic flux distribution in the magnetic core (Type B).

netic flux density over z-x plane which corresponds to the following notation,

$$\Phi(y) = \int_{\text{core}} B_{\text{n}}(y)\, dS. \tag{10}$$

The calculation results are shown in Fig. 26, where the magnetic flux is plotted against the distance from the center of magnetic core. Figure 26 illustrates that the magnetic flux has the maximum value at the center of the core, and decreases slowly with distance from the center to the winding width of the coil. The slope reveals a sudden change at the end of winding width. The reason for the steeper decrease of magnetic fluxes along the lead part is that the magnetic flux in the z-x plane becomes larger, as a result of small magnetic flux along the y axis. This is probably because of the incidence of magnetic flux from outside of the antenna core and lead parts which have large permeability.

The induced voltage for the receiving antenna in the resonance condition is given by

$$V_{\text{r}} = 2\pi f_0 \sum_{i=1}^{N} \phi_i Q = 2\pi f_0 N \gamma \phi_{\text{m}} Q, \tag{11}$$

where f_0, ϕ_{i}, Q, N, γ and ϕ_{m} represent the resonance frequency, the magnetic flux linking the ith turn, Q-factor, number of turns of the coil, the winding coefficient, and the maximum magnetic flux inside the coil. The terms γ and ϕ_{m}

depend on the shape of the antenna. The winding coefficient is defined as the ratio of averaged magnetic flux within the coil to that of the maximum magnetic flux, ϕ_{m}. To make larger receiving voltage it is desirable that the winding coefficient takes close to unity. The winding coefficient of the LF antenna is expressed as follows.

$$\gamma = \frac{\int_{\mathrm{coil}} \phi(y)\, dy/W}{\phi_m}, \tag{12}$$

where W is the winding width of the coil. A winding coefficient, $\gamma = 0.95$, was obtained by the simulation for MCLA used in the product (Type B, Fig. 13). It is reasonable to have a relatively large winding coefficient of 0.95 for antennas in the radio controlled watch, because it has lead parts of the magnetic body.

6. Conclusion

In this paper, we discussed the analysis of MCLAs. The major results are listed as follows:

(1) We presented the simulation model and the measurement method of MCLAs.
(2) The inductance of bar shaped MCLAs with various shape parameters was examined by measurement and simulation. Very good agreement was observed between measurement and simulation.
(3) We analyzed the inductance, the Q-factor and the antenna factor of an actual MCLA used in the products. The inductance and the Q-factor coincide with measured values, while for the antenna factor, the maximum difference between measured values and simulation results is 2 dB.
(4) We investigated the concentration of magnetic flux from the lead part of the MCLA by simulation. We have found that the trapezoidal pillar-shaped antenna is suitable for miniaturization and high sensitivity.

In summary, we are able to accurately evaluate the inductance, the Q-factor and the antenna factor of the MCLAs by the simulation.

In the future we plan to design MCLAs for radio controlled watches, taking into account the more realistic implementation issues such as the influence of a metal case.

References

[1] Japan Standard Time Group, http://jjy.nict.go.jp/
[2] H.J. Laurent and C.A.B. Carvalho, "Ferrite antennas for A.M. broadcast receivers," IRE Trans. Broadcast and Television Receivers, vol.8, no.2, pp.50–59, 1962.
[3] R.C. Pettengill, H.T. Garland, and J.D. Meindl, "Receiving antenna design for miniature receivers," IEEE Trans. Antennas Propag., pp.528–530, July 1977.
[4] J.D. Kraus and K.R. Carver, Electromagnetics, 2nd ed., pp.155–160, McGraw-Hill, New York, 1973.
[5] Ansoft Corporation, http://www.ansoft.com/
[6] ANSI/IEEE Std. 189–1955, "IEEE standard method of testing receivers employing ferrite core loop antennas," Institute of Electrical and Electronics Engineers, New York, 1955.
[7] K. Abe and J. Takada, "Performance simulation of LF receive antenna," Proc. IEICE Gen. Conf. 2005, B-1-151, March 2005.
[8] K. Abe and J. Takada, "Investigation about shape simulation of small LF antennas," Proc. Commun. Conf. IEICE, B-1-39, Sept. 2005.

Kazuaki Abe was born in Gunma, Japan in 1967. He received the B.S. and M.S. degrees in physics from University of Tsukuba, Tsukuba, Japan, in 1990 and 1992, respectively. He joined CASIO Computer Co., Ltd., Tokyo in 1992. His current research interest is LF antenna for radio controlled watches.

Jun-ichi Takada received the B.E., M.E., and D.E. degrees from the Tokyo Institute of Technology, Tokyo, Japan, in 1987, 1989, and 1992, respectively. From 1992 to 1994, he was a Research Associate Professor with Chiba University, Chiba, Japan. From 1994 to 2006, he was an Associate Professor with Tokyo Institute of Technology. Since 2006, he has been a Professor with Tokyo Institute of Technology. His current interests are wireless propagation and channel modeling, array signal processing, UWB radio, cognitive radio, applied radio instrumentation and measurements, and ICT for international development. Dr. Takada is a member of IEEE, ACES, and the ECTI Association Thailand.